Line Aging Assessment in Distribution Network Based on Topology Verification and Parameter Estimation

Zhi Wu, *Member*, *IEEE*, Huan Long, and Chang Chen

***Abstract*—The aging of lines has a strong impact on the economy and safety of the distribution network. This paper proposes a novel approach to conduct line aging assessment in the distribution network based on topology verification and parameter estimation. In topology verification, the set of alternative topologies is firstly generated based on the switching lines. The best-matched topology is determined by comparing the difference between the actual measurement data and calculated voltage magnitude curves among the alternative topologies. Then, a novel parameter estimation approach is proposed to estimate the actual line parameters based on the measured active power, reactive power, and voltage magnitude data. It includes two stages, i.e., the fixed-step aging parameter (FSAP) iteration, and specialized Newton-Raphson (SNR) iteration. The theoretical line parameters of the best-matched topology are taken as a warm start of FSAP, and the fitted result of FSAP is further renewed by the SNR. Based on the deviation between the renewed and theoretical line parameters, the aging severity risk level of each line is finally quantified through the risk assessment technology. Numerous experiments on the modified IEEE 33-bus and 123-bus systems demonstrate that the proposed approach can effectively conduct line aging assessment in the distribution network.**

***Index Terms*—Line aging, topology verification, parameter estimation, risk assessment, Newton-Raphson iteration.**

NOMENCLATURE

α, β	Iterative step coefficients of conductance and susceptance of fixed-step aging parameter (FSAP)
α_{TV}	Accuracy of topology verification
$\delta_g^\ell, \delta_b^\ell$	Conductance and susceptance offset of the ℓ^{th} line
ε_{pq}	Load measurement error
ε_v	Voltage magnitude measurement error
ℓ	Index of lines ($\ell = 1, 2, \ldots, N_\ell$)
λ_ℓ	Aging coefficient of unit resistance of the ℓ^{th} line
ρ	Similarity between alternative and actual topologies in topology verification
$\boldsymbol{\Phi}$	Theoretical line parameter profile
$\boldsymbol{\Psi}_{H,n}$, $\boldsymbol{\Psi}_{E,n}$	Sets of head buses and end buses of $\boldsymbol{\Psi}_n$
$\boldsymbol{\Psi}_n$	Set of connected switching lines in the n^{th} alternative grid topology
$\boldsymbol{\Omega}'$	Best-matched topology
$\boldsymbol{\Omega}_n$	Topology in the n^{th} alternative grid topology
g_ℓ, b_ℓ	Theoretical admittance of the ℓ^{th} line
$\hat{g}_\ell$, $\hat{b}_\ell$	Renewed line parameters
g_ℓ^a, b_ℓ^a	Actual admittance of the ℓ^{th} line
k	Index of connected switching lines in the n^{th} alternative grid topology ($k = 1, 2, \ldots, N_n$)
L_h	Length of hours selected for topology verification
n	Index of alternative grid topologies ($n = 1, 2, \ldots, N_{GT}$)
N_b	Number of buses of actual topology
N_c	Number of topologies that are correctly matched
N_{GT}	Number of alternative grid topologies
N_n	Number of connected switching lines in the n^{th} alternative grid topology
$\boldsymbol{P}^a$, $\boldsymbol{P}^c$	Actual and calculated active power injection data
$\boldsymbol{Q}^a$, $\boldsymbol{Q}^c$	Actual and calculated reactive power injection data
$S(\ell)$	Degree of abnormity severity of the ℓ^{th} line
t	Index of time slots ($t = 1, 2, \ldots, T$)
T_s	Sampling frequency of measurement data
$\boldsymbol{V}^a$, $\boldsymbol{V}^c$	Actual and calculated voltage magnitude data
V_{aw}	Aging warning value

Manuscript received: March 10, 2021; revised: October 27, 2021; accepted: October 27, 2021. Date of CrossCheck: October 27, 2021. Date of online publication: January 11, 2022.

This work was supported in part by National Natural Science Foundation of China (No. 51807023) and Natural Science Foundation of Jiangsu Province (No. BK20180382).

Z. Wu and H. Long (corresponding author) are with the School of Electrical Engineering, Southeast University, Nanjing, China (e-mail: zwu@seu. edu. cn; hlong@seu.edu.cn).

C. Chen is with Maintenance Branch Company, State Grid Jiangsu Electric Power Company Ltd., Nanjing, China (e-mail: freja86@163.com).

DOI: 10.35833/MPCE.2021.000165

I. INTRODUCTION

THE lines in the power grid have a limited service life and inevitable aging due to various factors such as hydrolysis, oxidation, and pyrolysis [1]. The aging of lines has a harmful impact on the distribution network, which can be reflected in system reliability and state estimation. If the aging lines in the distribution network are not replaced in time, their insulation layer may be destroyed during power transmission. It seriously affects the normal power supply and causes substantial economic losses [2]-[4]. Thus, line aging assessment and localization in the distribution network are essential to enhance the system reliability and ensure the economic benefit of electric power companies.

References [5]-[9] on line aging assessment mainly focus on the modeling and the influencing factor. In [7], a 10 kV distribution line aging mathematical model is established. The impedance changes of various lines with different operating years are fitted based on actual measurement data. The equivalent resistance method is used to analyze the effect of line aging on the power loss in the distribution network. In [8], several long-term operating and aging conductors are taken as the samples. Time-temperature experiments are conducted to evaluate the current carrying capacity and resistivity. The deviation degree of line parameters can be used to measure the aging degree of lines. In [10], a novel methodology is proposed for spatial analysis of thermal aging of overhead transmission conductors, which could be performed at three different levels: point, line, and area. In [11], a novel method is proposed to calculate the aging failure probability of power transmission lines based on the dynamic heat balance equation and Weibull distribution. However, the experiments of the above modeling methods are complicated and time-consuming, and many actual environmental impact factors are ignored. Moreover, since the line aging assessment is only conducted for individual lines, these methods fail to locate the aging lines in the actual distribution network.

Thus, to deal with the actual situation, the actual information of the grid topology and line parameters is the premise of locating the aging lines in the distribution network. It is noted that the topology of the distribution network is usually changed through the switching lines to optimize the network operation [12]. It brings great difficulties in obtaining accurate topology information. Fortunately, with the development of the smart grid, massive operation data are continuously generated, which provide a basis to achieve the actual topology and line parameters.

Currently, the actual topology can be achieved based on topology verification [13]-[16] or topology identification [17]-[20]. In topology verification, the existing line infrastructure and the theoretical line parameters can be obtained. The actual topology is determined based on alternative operating structures and the actual operating measurement data. In [13], a meter placement strategy is developed to allow distribution system operators to deploy only a few real-time meters, ensuring unique recovery of the true distribution network topology in real time. In [14], a voting-based topology detection method is presented, working with active power, reactive power, voltage magnitude, and voltage phase angle data. In [15], a statistical learning framework is put forth for verifying grid structures using active power, reactive power, and non-synchronized voltage angle data. In [16], a sensor placement strategy is proposed to identify the energized grid topology by exploiting real-time active power, reactive power, and voltage magnitude data collected at partial buses. Different from the topology verification, the task of topology identification is to find both the line connections and line parameters. In [17], the error-in-variables model in a maximum-likelihood estimation framework for joint line parameter and topology estimation is proposed. The PaToPa approach uses a full set of active and reactive power, voltage magnitude, and voltage phase angle data to estimate the parameters. In [18], a two-step framework is developed to identify the topology and estimate line parameters with the active power, reactive power, and voltage magnitude data. The specialized Newton-Raphson (SNR) is proposed to use the pseudo power calculation without the voltage phase angle data to estimate the line parameters. In [19], smart inverters are employed to perturb the distribution network to actively infer its topology and estimate line parameters. In [20], a mixed-integer linear programming method is employed based on McCormick relaxation for the topology identification of distribution network using inverter probing.

The above topology identification methods [17]-[20] not only recover the actual topology structure, but also estimate line parameters. However, they need the voltage angle data or require high measurement accuracy, which causes great measurement costs. In most cases, the theoretical topology profile can be obtained. Thus, the topology verification without voltage angle measurement data is considered. Since the SNR [18] is sensitive to the voltage magnitude measurement error, it is easy to be trapped in the non-convergence problem. The fixed-step aging parameter (FSAP) algorithm is proposed in this paper to estimate the line parameters, which can be the initial value of SNR to improve its robustness of the measurement noise.

After topology verification, it is also a key point to measure the aging degree of all lines in the distribution network to locate the specific aging line and send the aging warning. In this paper, the risk assessment technology of the distribution network is employed to measure the line aging risk severity level. The risk assessment has been gradually applied to various power industry areas, mainly including operational risk monitoring, equipment management, etc. [21]-[24]. In [22], the risk assessment technology is utilized to quantify the stability degree of power system under hidden faults and cascading faults. In [23], a hierarchical risk assessment method is introduced to properly consider the impacts of active distribution networks on the risk analysis of the transmission system. The values of line parameters can directly reflect the impact of aging lines [8]. Thus, the risk assessment is suitable for line aging assessment to locate the aging lines based on the reasonable severity utility function.

In this paper, a novel approach for line aging assessment is proposed, which consists of three parts, i.e., topology verification, parameter estimation, and line aging assessment. The alternative topologies are generated based on the different connections of switching lines. Based on voltage magnitude and power injection data, the best-matched topology is selected by comparing the actual voltage magnitude curves with the calculated ones of the alternative topologies. The theoretical line parameters of the best-matched topology are taken as a warm start of line parameter estimation. The line parameters are renewed to best fit the actual measurement data based on the proposed FSAP-SNR iteration method, which reduces the high requirements of voltage magnitude measurement of SNR in [18]. To further assess the aging lines, the aging severity risk level of each line is quantified based on the deviation between the renewed and theoretical line parameters. The main contributions of this paper can be concluded as follows.

1) The framework of line aging assessment in the distribution network is proposed.

2) A new parameter estimation approach, FSAP-SNR iteration, is proposed, which only requires the voltage magnitude and active and reactive power measurement data, and is robust for the measurement noise.

3) A severity utility function based on the admittance is developed for line aging assessment.

The remainder of this paper is as follows. Section II introduces the structure and details of the proposed approach. Section III presents the case study by using the proposed approach based on the modified IEEE 33-bus and IEEE 123-bus systems. The conclusion and future work are given in Section IV.

II. Structure and Details of Proposed Approach

In this section, the structure and details of the proposed approach are presented, and the details of each part are described later.

A. Structure of Proposed Approach

The proposed line aging assessment approach in the distribution network is composed of topology verification, parameter estimation, and line aging assessment, as presented in Fig. 1. In the stage of topology verification, the alternative network topology set is firstly generated based on the switching lines. The best-matched topology is then selected based on the difference of actual and calculated voltage magnitudes. In the stage of parameter estimation, the actual line parameters of the best-matched topology are estimated based on the proposed FSAP-SNR iteration. In the stage of line aging assessment, the aging severity risk level of each line is assessed based on the proposed severity utility function by comparing the deviation of the estimated and theoretical line parameters. The aging lines are finally detected based on the values of the severity utility function.

B. Topology Verification

The purpose of topology verification is to determine the best-matched topology among different possible topologies by minimizing the difference between the actual and calculated voltage magnitudes. A pseudo-code of the topology verification algorithm is provided in Algorithm 1.

Assume that a radial distribution grid with N_b buses can be admitted to operate with N_{GT} alternative grid topologies due to the different connected switching lines. The theoretical line parameter profile $\boldsymbol{\Phi}$ includes conductance and susceptance. The measured data over T time instances include the voltage magnitude $\boldsymbol{V}^a=\{\boldsymbol{V}_t^a, t=1,2,\dots,T\}$, active power injection $\boldsymbol{P}^a=\{\boldsymbol{P}_t^a, t=1,2,\dots,T\}$, and reactive power injection, $\boldsymbol{Q}^a=\{\boldsymbol{Q}_t^a, t=1,2,\dots,T\}$. In the n^{th} alternative grid topology, the calculated voltage magnitude, $\boldsymbol{V}_n^c=\{\boldsymbol{V}_{t,n}^c, t=1,2,\dots,T\}$, is obtained by power flow calculation $f(\cdot)$ (line 2 to line 4). Considering that the fluctuation degree of voltage magnitude is mainly related to the node injection and grid topology, the smallest difference between $\boldsymbol{V}^a$ and $\boldsymbol{V}_n^c$ can infer the best-matched topology. By comparing the similarity of fluctuation of $\boldsymbol{V}^a$ and $\boldsymbol{V}_n^c$ at the buses in $\boldsymbol{\Psi}_n$, the best-matched topology $\boldsymbol{\Omega}'$ is obtained, which is considered as the actual topology (line 5 to line 8).

C. Parameter Estimation

In order to further detect and locate the aging lines in the best-matched topology $\boldsymbol{\Omega}'$, the actual line parameter profile of the topology $\boldsymbol{\Omega}'$ is estimated based on the measurement data $\boldsymbol{V}^a$, $\boldsymbol{P}^a$, and $\boldsymbol{Q}^a$. This paper proposes a novel parameter estimation approach, FSAP-SNR, which is robust to the measurement noise without the information of voltage phase angle. It should be noted that the FSAP algorithm renews the line parameters by the fixed step, which is suitable for the small distribution network. In large-scale distribution network, the SNR algorithm is utilized to further renew the parameters based on the result of FSAP. The flowchart of parameter estimation is shown in Fig. 2.

1) FSAP

The FSAP algorithm is a parameter estimation algorithm with the fixed iteration step. Considering that the voltage magnitude measurement error ε_v is usually smaller than the load measurement error ε_{pq} in the actual distribution system, the FSAP algorithm selects voltage magnitude as the iterative convergence condition to guarantee the robustness. A pseudo-code of the FSAP algorithm is provided in Algorithm 2.

Let $g_\ell+\mathrm{j}b_\ell$ and $g_\ell^a+\mathrm{j}b_\ell^a$ be the theoretical and actual admittance of the ℓ^{th} line ($\ell=1,2,\dots,N_\ell$), respectively. Renew g_ℓ and b_ℓ based on the corresponding Δg_ℓ and Δb_ℓ, as shown in line 1 in Algorithm 2. The power flow calculation $f(\cdot)$ is then employed to calculate the voltage magnitudes $\boldsymbol{V}^c$ of all buses based on the topology $\boldsymbol{\Omega}'$, renewed line parameters $\{\hat{g}_\ell, \hat{b}_\ell\}$, $\boldsymbol{P}^a$, and $\boldsymbol{Q}^a$. The sum of voltage magnitude differences ΔV of all buses over T time slots is compared with the pre-setting threshold σ. When ΔV is smaller than σ, the corresponding $\hat{g}_l$ and $\hat{b}_l$ are considered as the best estimates.

Based on Algorithm 2, it is clear that the iterative direction of each line, $\mathrm{sgn}(g_\ell^a-g_\ell)$ and $\mathrm{sgn}(b_\ell^a-b_\ell)$, are essential for the performance of estimation.

Since the value of the resistance inevitably increases in the aging lines and the values of the reactance of lines are small, $\mathrm{sgn}(g_\ell^a-g_\ell)$ and $\mathrm{sgn}(b_\ell^a-b_\ell)$ can be obtained by the relationship between resistance and reactance.

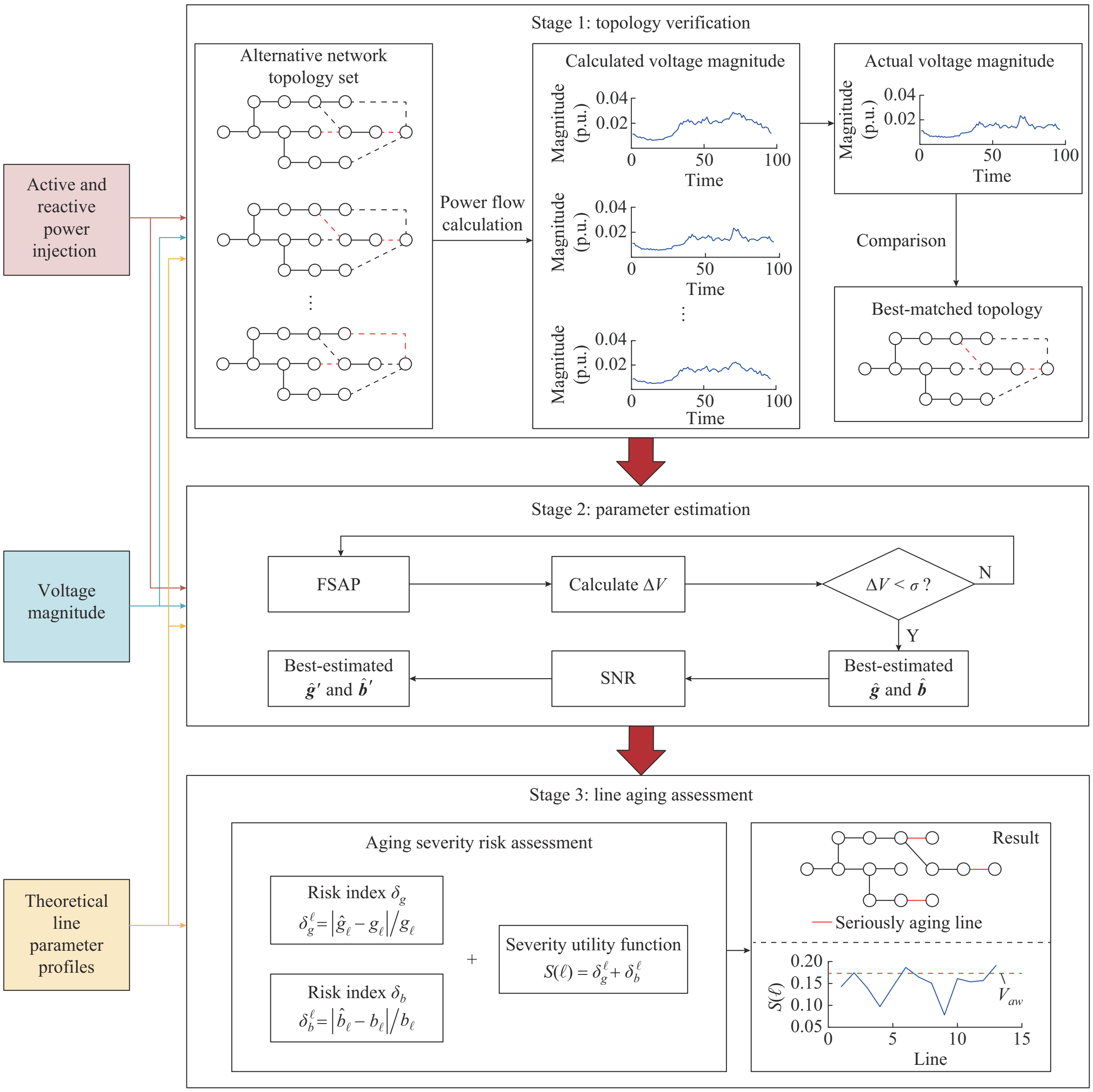

Fig. 1. Flowchart of proposed line aging assessment approach.

Algorithm 1: topology verification

Input: given datasets $\boldsymbol{V}^a$, $\boldsymbol{P}^a$, $\boldsymbol{Q}^a$, $\boldsymbol{\Phi}$, $\boldsymbol{\Omega}_n$, and $\boldsymbol{\Psi}_n$, $n=1,2,\ldots,N_{GT}$

Output: best-matched grid topology $\boldsymbol{\Omega}'$

for $n \leftarrow 1$ to N_{GT} **do**

  for $t \leftarrow 1$ to T **do**

    $V_{t,n}^c = f(\boldsymbol{\Omega}_n, \boldsymbol{\Phi}, \boldsymbol{P}_t^a, \boldsymbol{Q}_t^a)$

  end for

$$\rho(n) = \frac{1}{1 + \dfrac{1}{TN_n}\sqrt{\sum_{t=1}^{T}\sum_{k=1}^{N_n}\left[(V_{t,n,\psi_{H,n,k}}^c - V_{t,n,\psi_{E,n,k}}^c) - (V_{t,n,\psi_{H,n,k}}^a - V_{t,n,\psi_{E,n,k}}^a)\right]^2}}$$

end for

$\boldsymbol{\Omega}' = \boldsymbol{\Omega}_{\mathrm{argmax}(\rho)}$

return $\boldsymbol{\Omega}'$

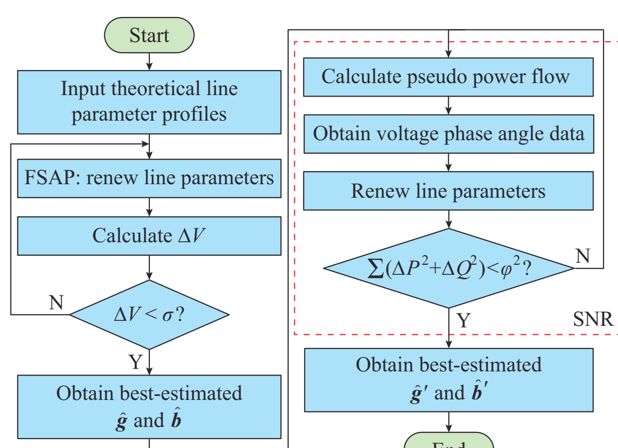

Fig. 2. Flowchart of parameter estimation.

Algorithm 2: FSAP

Input: given dataset $\boldsymbol{V}^a$, $\boldsymbol{P}^a$, $\boldsymbol{Q}^a$, $\boldsymbol{\Phi}=\{g_\ell, b_\ell\}$ $(\ell \in \boldsymbol{\Omega}')$, $\boldsymbol{\Omega}'$, α, β, and σ

Output: best estimated $\hat{\boldsymbol{g}}$ and $\hat{\boldsymbol{b}}$

```
Δg_ℓ = α g_ℓ · sgn(g_ℓ^a − g_ℓ), Δb_ℓ = β b_ℓ · sgn(b_ℓ^a − b_ℓ)
while ΔV ≥ σ do
    ĝ_ℓ = ĝ_ℓ + Δg_ℓ, b̂_ℓ = b̂_ℓ + Δb_ℓ
    for t ← 1 to T do
        V_t^c = f(Ω', ĝ, b̂, P_t^a, Q_t^a)
    end for
    ΔV = 1/(T N_b) Σ_{t=1}^{T} Σ_{i=1}^{N_b} |V_{t,i}^c − V_{t,i}^a|
end while
return ĝ and b̂
```

It is assumed that the theoretical and actual impedances of the ℓ^{th} line ($\ell \in \boldsymbol{\Omega}'$) satisfy $r_\ell^a=\lambda_\ell r_\ell$ ($\lambda_\ell>1$) and $x_\ell^a=x_\ell$. The difference between $g_\ell(b_\ell)$ and $g_\ell^a(b_\ell^a)$ is given in (1) and (2).

$$g_\ell^a-g_\ell=\operatorname{Re}\left(\frac{1}{r_\ell+\mathrm{j}x_\ell}\right)-\operatorname{Re}\left(\frac{1}{r_\ell^a+\mathrm{j}x_\ell^a}\right)=\frac{r_\ell(\lambda_\ell-1)(x_\ell^2-\lambda_\ell r_\ell^2)}{(\lambda_\ell^2 r_\ell^2+x_\ell^2)(r_\ell^2+x_\ell^2)} \tag{1}$$

$$b_\ell^a-b_\ell=\operatorname{Im}\left(\frac{1}{r_\ell+\mathrm{j}x_\ell}\right)-\operatorname{Im}\left(\frac{1}{r_\ell^a+\mathrm{j}x_\ell^a}\right)=\frac{x_\ell r_\ell^2(\lambda_\ell^2-1)}{(\lambda_\ell^2 r_\ell^2+x_\ell^2)(r_\ell^2+x_\ell^2)} \tag{2}$$

In (2), it is obvious that $\operatorname{sgn}(b_\ell^a-b_\ell)=1$ due to $\lambda_\ell>1$. In (1), three conditions can be discussed as follows.

1) If $x_\ell \le r_\ell$, then $\operatorname{sgn}(g_\ell^a-g_\ell)=-1$.

2) If $x_\ell>r_\ell$ and $1<\lambda_\ell<x_l^2/r_l^2$, then $\operatorname{sgn}(g_\ell^a-g_\ell)=1$.

3) If $x_\ell>r_\ell$ and $\lambda_\ell>x_l^2/r_l^2$, then $\operatorname{sgn}(g_\ell^a-g_\ell)=-1$.

2) SNR Iteration

Since FSAP is a parameter estimation algorithm with fixed iterative step size, it is difficult to select the suitable iterative step size in large-scale distribution network. The SNR algorithm proposed in [18], which is an iteration approach with variable step size, is used to further renew the line parameters based on the results of FSAP. The data requirement of SNR is the same as that of FSAP, including voltage magnitude and active/reactive power injection data.

A pseudo-code of SNR is provided in Algorithm 3. Since the voltage angle measurement is unavailable, the SNR first utilizes the pseudo-power flow calculation to estimate the voltage phase angle data in [18]. In the pseudo-power flow calculation, all the buses (except reference bus) are regarded as *PQ* nodes. The missing voltage phase angle $\boldsymbol{\Theta}$ are estimated based on $\boldsymbol{P}^a$, $\boldsymbol{Q}^a$, $\hat{\boldsymbol{g}}'$, and $\hat{\boldsymbol{b}}'$ through the pseudo-power flow calculation $\boldsymbol{pf}(\cdot)$. The initial $\hat{\boldsymbol{g}}'$ and $\hat{\boldsymbol{b}}'$ come from the results of FSAP.

Then, $\hat{\boldsymbol{g}}'$ and $\hat{\boldsymbol{b}}'$ are updated according to (3):

$$\begin{bmatrix}\Delta\boldsymbol{g}'\\ \Delta\boldsymbol{b}'\\ \Delta\boldsymbol{\Theta}'\end{bmatrix}=\begin{bmatrix}\dfrac{\partial\boldsymbol{P}}{\partial\boldsymbol{g}} & \dfrac{\partial\boldsymbol{P}}{\partial\boldsymbol{b}} & \dfrac{\partial\boldsymbol{P}}{\partial\boldsymbol{\Theta}}\\ \dfrac{\partial\boldsymbol{Q}}{\partial\boldsymbol{g}} & \dfrac{\partial\boldsymbol{Q}}{\partial\boldsymbol{b}} & \dfrac{\partial\boldsymbol{Q}}{\partial\boldsymbol{\Theta}}\end{bmatrix}^{\dagger}\begin{bmatrix}\Delta\boldsymbol{P}\\ \Delta\boldsymbol{Q}\end{bmatrix}=\begin{bmatrix}\boldsymbol{A} & \boldsymbol{B} & \boldsymbol{C}\\ \boldsymbol{D} & \boldsymbol{E} & \boldsymbol{F}\end{bmatrix}^{\dagger}\begin{bmatrix}\Delta\boldsymbol{P}\\ \Delta\boldsymbol{Q}\end{bmatrix} \tag{3}$$

where † represents generalized inverse. The partitioned matrices $\boldsymbol{A}$, $\boldsymbol{B}$, $\boldsymbol{D}$, and $\boldsymbol{E}$ are the power-branch partitioned matrices. $\boldsymbol{C}$ and $\boldsymbol{F}$ are the power-angle partitioned matrices. The details of partitioned matrices and the generalized inverse of Jacobian matrix calculation based on multiple samples can be referred in [18].

Algorithm 3: SNR

Input: given dataset $\boldsymbol{V}^a$, $\boldsymbol{P}^a$, $\boldsymbol{Q}^a$, $\boldsymbol{\Omega}'$, $\hat{\boldsymbol{g}}$, $\hat{\boldsymbol{b}}$, and φ^2

Output: best-estimated $\hat{\boldsymbol{g}}'$ and $\hat{\boldsymbol{b}}'$

```
ĝ' = ĝ, b̂' = b̂
while ΔS ≥ φ^2 do
    Θ = pf(Ω', ĝ', b̂', P^a, Q^a)
    [Δg'; Δb'; ΔΘ'] = [A B C; D E F]^† [ΔP; ΔQ]
    [ĝ'; b̂'] = [ĝ'; b̂'] + [Δg'; Δb']
    ΔS = 1/(T N_b) Σ_{i=1}^{T N_b} (ΔP_i^2 + ΔQ_i^2)
end while
return ĝ' and b̂'
```

The convergence criterion of the SNR is the sum of squares of the deviation between the actual and calculated values of the load power smaller than the pre-setting threshold φ^2.

It should be noted that the SNR is sensitive to the voltage magnitude measurement data. If SNR is employed alone based on the theoretical line parameter profile, the SNR may suffer non-convergence when ε_v is large. The estimated results of FSAP provide a good initial solution for SNR to benefit its convergence. Thus, the FSAP can be conducted alone, which is suitable for the small-scale distribution network, and the FSAP-SNR is preferred in large-scale distribution network.

Significantly, the step size of SNR can also provide an alternative choice for FSAP to guarantee its convergence performance. To simultaneously conduct the FSAP and SNR based on the initial theoretical line parameters, the step size of FSAP is determined by $\min\{\Delta\boldsymbol{g}, \Delta\boldsymbol{g}'\}$ and $\min\{\Delta\boldsymbol{b}, \Delta\boldsymbol{b}'\}$ in each iteration.

D. Aging Line Risk Assessment

In this subsection, the aging severity risk level of each line is quantified to assess the aging lines in the distribution network. The aging lines with obsolete equipment can easily cause grid failures and affect the stable operation and economic benefits of the distribution network, which is reflected in the variation of line parameters. Two risk indexes are constructed, i.e., the conductance offset δ_g^ℓ, and the susceptance offset δ_b^ℓ, in the topology $\boldsymbol{\Omega}'$, which significantly impacts the aging degree of each line ℓ, as expressed in (4).

$$\begin{cases}\delta_g^\ell=\left|\hat{g}_\ell-g_\ell\right|/g_\ell\\ \delta_b^\ell=\left|\hat{b}_\ell-b_\ell\right|/b_\ell\end{cases} \tag{4}$$

In order to measure the aging severity risk level of each line ℓ, the severity utility function is utilized as (5), which represents that the degree of abnormity severity increases with the sum of δ_g^l and δ_b^l.

$$S(\ell)=\delta_g^\ell+\delta_b^\ell \tag{5}$$

III. Case Study

The performance of the proposed approach, including topology verification, parameter estimation, and line aging assessment, is validated in the modified IEEE 33-bus and IEEE 123-bus systems in this section.

A. Data Description

The topology structures of modified IEEE 33-bus and IEEE 123-bus systems with 10 and 14 switching lines, are illustrated in Fig. 3 and Fig. 4, respectively.

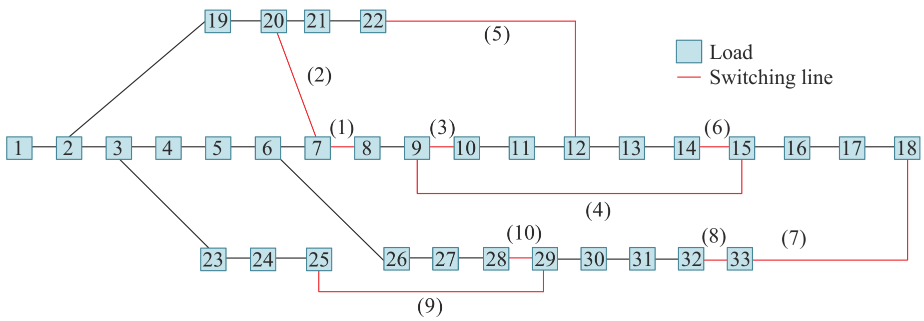

Fig. 3. Topology structure of modified IEEE 33-bus system.

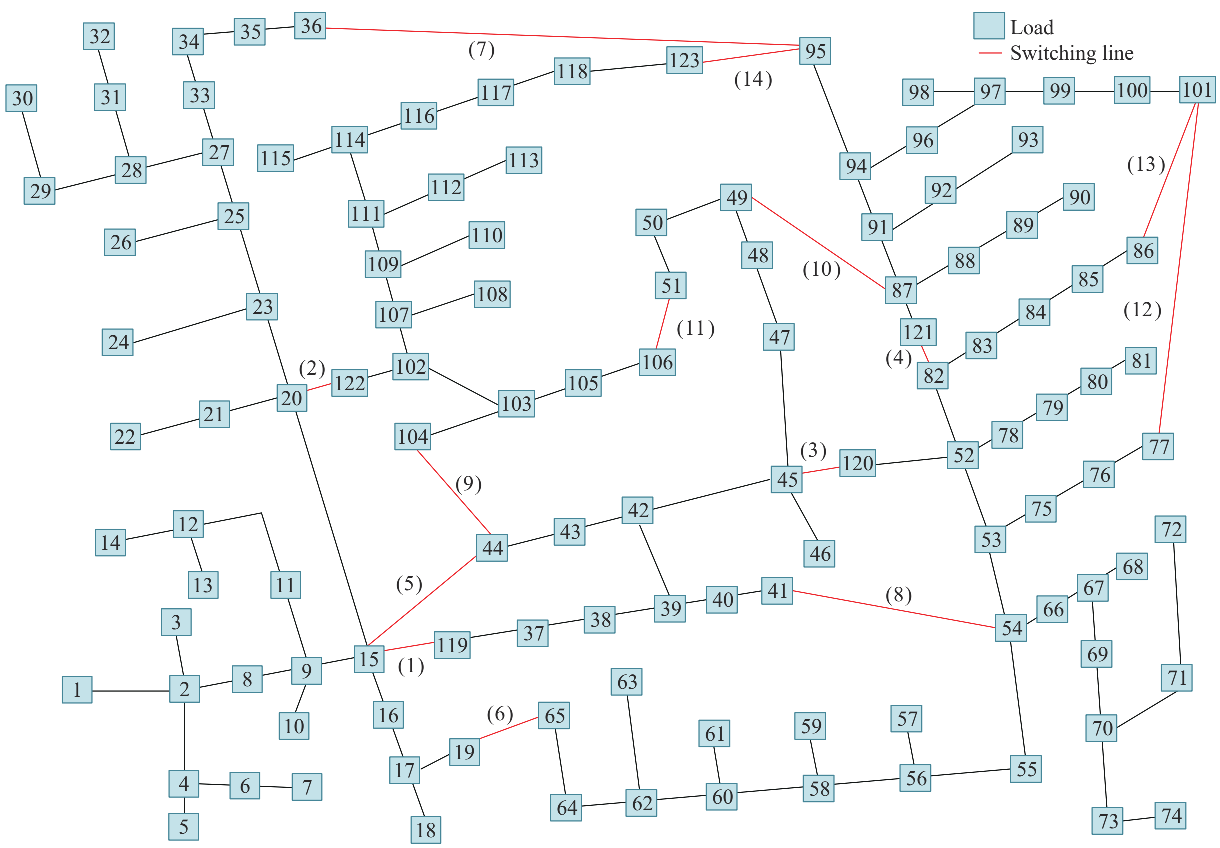

Fig. 4. Topology structure of modified IEEE 123-bus system.

To simulate aging of lines, the unit resistance of the aged conductors is increased by 4%-14% compared with the new ones in the IEEE 33-bus and 123-bus systems based on [8]. Thus, λ_ℓ is randomly set to be 1.04-1.14 for line ℓ. In this paper, the active and reactive load profiles for power consumers sampled per 5 min are collected from Tianjin Electric Power Company in China on March 1, 2019. The voltage magnitude is obtained through power flow calculation based on the above load profiles and simulated aging line parameters.

Furthermore, to simulate the measurement error in the actual distribution network, the measurement noise of the load and voltage magnitude profiles are modeled by zero-mean Gaussian with a 3-sigma deviation matching ε_{pq} and ε_v of the original values, respectively. Take the modified IEEE 33-bus system as an example. The value of λ_ℓ is set to be 1.14. The relative errors between g_ℓ^a and g_ℓ^b, and b_ℓ^a and b_ℓ^b are shown in Fig. 5(a). ε_{pq} and ε_v are set to be 5% and 0.5%, respectively, as an example. The relative errors of loads and voltages between the values with measurement noise are presented in Fig. 5(b) and (c), respectively.

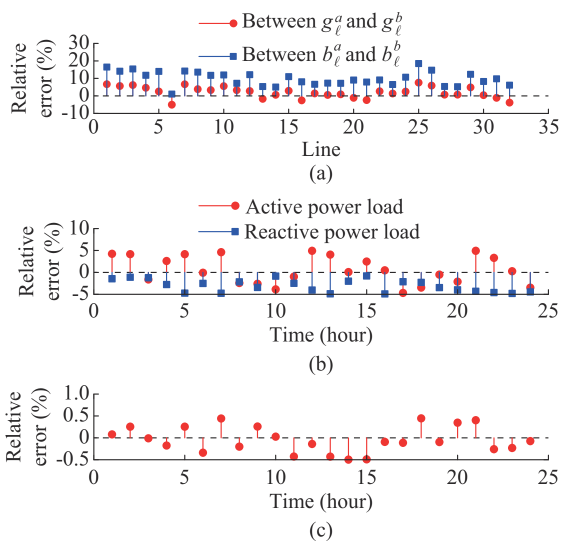

Fig. 5. Relative errors of line parameters, load, and voltage magnitude. (a) Line parameters. (b) Load. (c) Voltage magnitude.

B. Line Aging Assessment on Modified IEEE 33-bus System

1) Topology Verification

The accuracy of topology verification, α_{TV}, is evaluated by:

$$\alpha_{TV}=\frac{N_c}{N_{GT}}\times 100\% \tag{6}$$

Based on the switching lines, the modified IEEE 33-bus system in Fig. 3 has 87 alternative topologies. The switching lines (1), (3), (6), (8), and (10) in Fig. 3 are set to be connected, and the rest of the switching lines to be disconnected, and this topology is assumed to be the actual topology $\boldsymbol{\Omega}'$. The parameters are set to be $\varepsilon_{pq}=5\%$, $\varepsilon_v=0.5\%$, and $\lambda_\ell=1.14$. The sampling frequency T_s is set to be 15 min. In this case, ρ of each alternative topology structure is depicted in Fig. 6. In Fig. 6, each circle represents ρ of the corresponding alternative topology structure. It is clear that the 1st topology structure with the largest ρ is regarded as the best-matched topology.

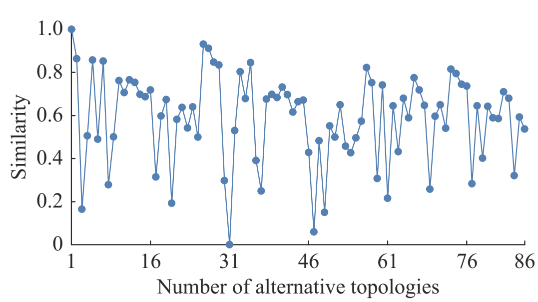

Fig. 6. ρ of each alternative topology structure in modified IEEE 33-bus system.

The sensitivity analysis of the effects of ε_{pq}, ε_v, and λ_ℓ on α_{TV} is also conducted. In this paper, the default settings of topology verification are $\varepsilon_{pq}=5\%$, $\varepsilon_v=0.5\%$, $\lambda_\ell=1.14$, and $T_s=15$ min. The result of sensitivity analysis with varying settings is depicted in Fig. 7. When ε_{pq} is less than 10%, α_{TV} is stable and more than 90%. Once ε_{pq} exceeds 10%, α_{TV} drops rapidly. Compared with the effect of ε_{pq} on α_{TV}, ε_v within the normal measurement error range has a more obvious impact on α_{TV}. The smaller ε_v is, the higher α_{TV} will be. λ_ℓ changes from 1.04 to 1.36 with the step size of 0.04, and α_{TV} also decreases accordingly.

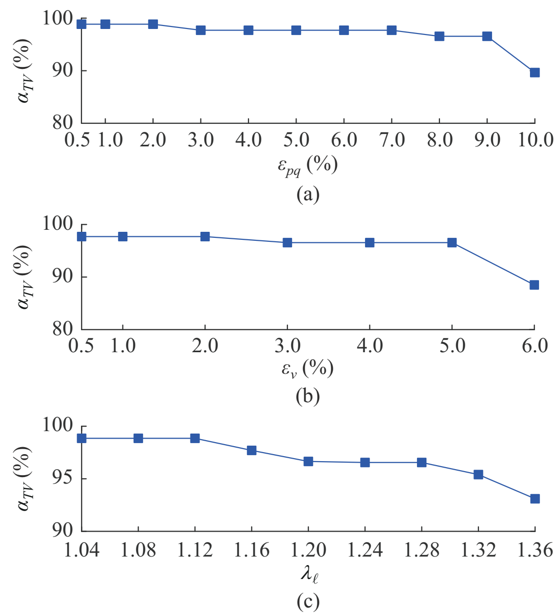

Fig. 7. Result of sensitivity analysis with varying settings. (a) ε_{pq}. (b) ε_v. (c) λ_ℓ.

2) Parameter Estimation

The validity of FSAP and FSAP-SNR is evaluated by the mean absolute percentage error (MAPE) of conductance g and susceptance b, as shown in (7) and (8), respectively.

$$MAPE(g)=\frac{1}{N_\ell}\sum_{\ell\in\boldsymbol{\Omega}'}\left|\frac{\hat{g}_\ell-g_\ell^a}{g_\ell^a}\right|\times 100\% \tag{7}$$

$$MAPE(b)=\frac{1}{N_\ell}\sum_{\ell\in\boldsymbol{\Omega}'}\left|\frac{\hat{b}_\ell-b_\ell^a}{b_\ell^a}\right|\times 100\% \tag{8}$$

The settings of parameter estimation are given as $\varepsilon_{pq}=5\%$, $\varepsilon_v=0.5\%$, $\lambda_\ell=1.14$, $T_N=10$, $\alpha=0.1$, $\beta=0.22$, and $T_s=15$ min. The objective function error in each iteration is presented in Fig. 8. The FSAP-SNR takes 55 iterations until convergence, and the final values of $MAPE(g)$ and $MAPE(b)$ are 2.344% and 3.212%, respectively. The best estimates and relative error between the renewed and actual values of line parameters of each line are shown in Fig. 9.

In order to further verify the validity of the proposed approach for parameter estimation in this paper, the comparison experiments of FSAP, FSAP-SNR, and SNR are conducted with varying values of ε_{pq}, which are set to be 0.5%, 1.0%, 3.0%, and 5.0%, respectively. The result is presented in Table I, where the SNR algorithm based on the initial parameter profiles needs high measurement accuracy of voltage and fails to converge when $\varepsilon_v \geq 0.5\%$. Thus, the results of SNR are not given in Table I. When ε_{pq} is small, the FSAP-SNR has better results than the FSAP. The FSAP enables the parameter estimation to reach a good result, and then the SNR fine-tunes the parameters to achieve more accurate result. However, when ε_{pq} increases, the SNR makes the estimation result worse. This is because the convergence condition of the SNR is that the sum of ΔP^2 and ΔQ^2 should be smaller than φ^2. When ε_{pq} is large, the parameter estimation may deviate the real values to meet the convergence condition. Thus, the parameter estimation accuracy of FSAP is acceptable for the simple distribution network.

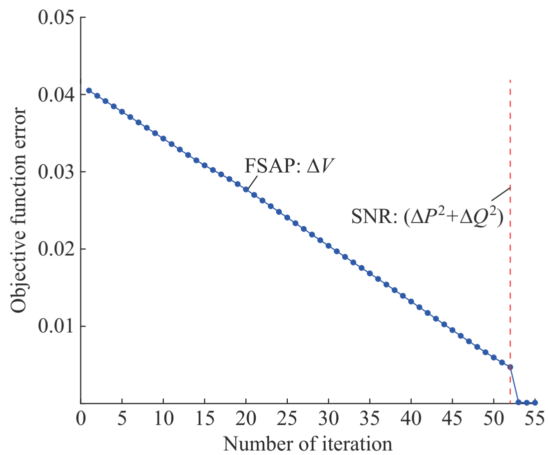

Fig. 8. Objective function error in each iteration.

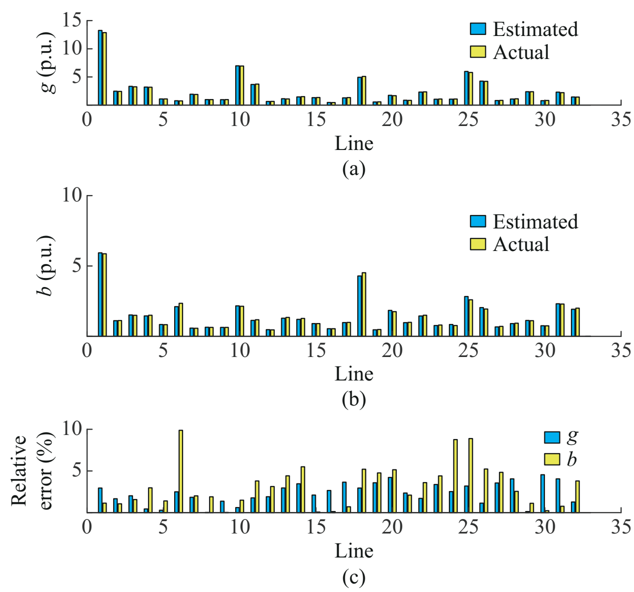

Fig. 9. Best estimates and relative error between renewed and actual values of line parameters of each line in modified IEEE 33-bus system. (a) Conductance. (b) Susceptance. (c) Relative error.

3) Line Aging Assessment

To assess the aging severity of each line in the modified topology in Fig. 3, the risk assessment is employed based on the determined topology and renewed line parameters.

TABLE I

RESULT OF COMPARISON EXPERIMENTS IN MODIFIED IEEE 33-BUS SYSTEM

ε_{pq} (%)	FSAP		FSAP-SNR	
	MAPE(g)	*MAPE(b)*	*MAPE(g)*	*MAPE(b)*
0.5	2.466	3.594	2.344	3.212
1.0	2.517	3.616	2.396	3.379
3.0	2.535	3.678	2.493	4.399
5.0	2.597	3.988	3.222	6.695

The result of line aging assessment is shown in Fig. 10. The more serious the line aging, the higher the δ_g^l, δ_b^l, and $S(\ell)$. The distribution network operators can set the aging warning value V_{aw} according to the actual situation. If $S(\ell)$ exceeds V_{aw}, the electric power company should replace the line ℓ as soon as possible. In this paper, V_{aw} is set to be 0.18. As presented in Fig. 10, there are 5 lines exceeding V_{aw}, which needs to be alerted.

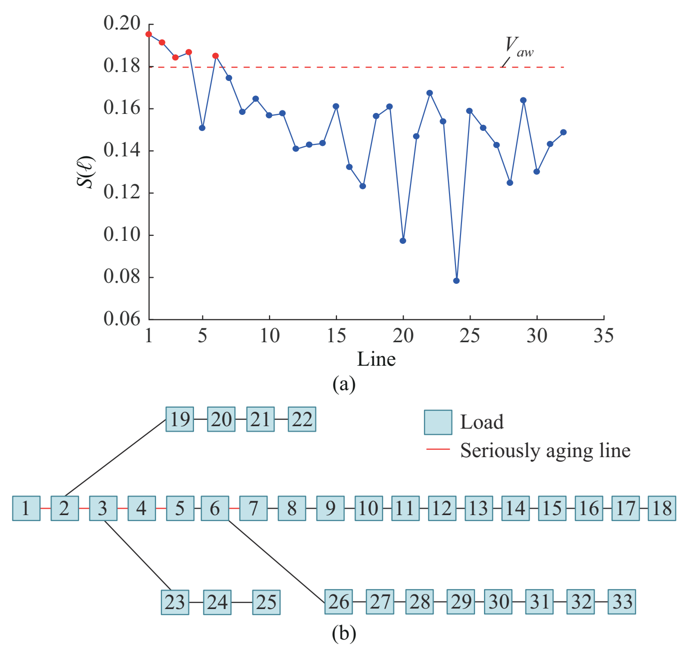

Fig. 10. Result of line aging assessment of modified IEEE 33-bus system. (a) $S(\ell)$. (b) Topology structure.

C. Line Aging Assessment on Modified IEEE 123-bus System

The proposed method is further conducted on the modified IEEE 123-bus system to validate its performance on the complex distribution network.

1) Topology Verification

Based on the switching lines in the modified IEEE 123-bus system in Fig. 4, it has 161 alternative topologies. The switching lines (1), (2), (3), (4), (6), and (14) in Fig. 4 are set to be connected, and the rest of the switching lines are set to be disconnected, and this topology is assumed as the actual topology $\boldsymbol{\Omega}'$. The default settings of topology verification are the same as those of the IEEE 33-bus system. In this case, ρ of each alternative topology is depicted in Fig. 11. The topology with the highest value of ρ is the best-matched topology.

The sensitivity analysis of the effects of ε_{pq}, ε_v, λ_ℓ, T_s, and the length of hours selected for topology verification L_h on α_{TV} is conducted. The default settings are $\varepsilon_{pq}=5\%$, $\varepsilon_v=0.5\%$, $\lambda_\ell=1.14$, $T_s=15$ min, and $L_h=2$. The result of the sensitivity analysis with varying settings is depicted in Fig. 12. Like the IEEE 33-bus system, α_{TV} falls with the increase of ε_{pq}, ε_v, and λ_ℓ. When $L_h=1$ and $T_s=1$ hour, α_{TV} is 90.683%. As the sample size is too small and only one sample is used in topological verification, the result is random and inaccurate. As L_h is set between 2 and 7, T_s and L_h do not have particularly obvious effects on α_{TV}, which are stable between 93% and 94%. When L_h is larger than 7, the lower T_s, the lower α_{TV}. The reason is that too many samples may bring in large measurement errors, which leads to inaccurate results of topology verification.

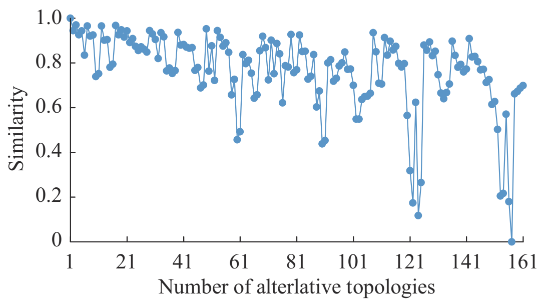

Fig. 11. ρ of each alternative topology in modified IEEE 123-bus system.

2) Parameter Estimation

Take the topology structure in Fig. 4 as an example. The settings of parameter estimation are $\varepsilon_{pq}=5\%$, $\varepsilon_v=0.5\%$, $\lambda_\ell=1.14$, $\alpha=0.05$, $\beta=0.19$, and $T_s=30$ min. The final values of $MAPE(g)$ and $MAPE(b)$ are 2.577% and 3.199%, respectively. The best estimates of line parameters and relative error between the renewed and actual values of line parameters of each line are shown in Fig. 13.

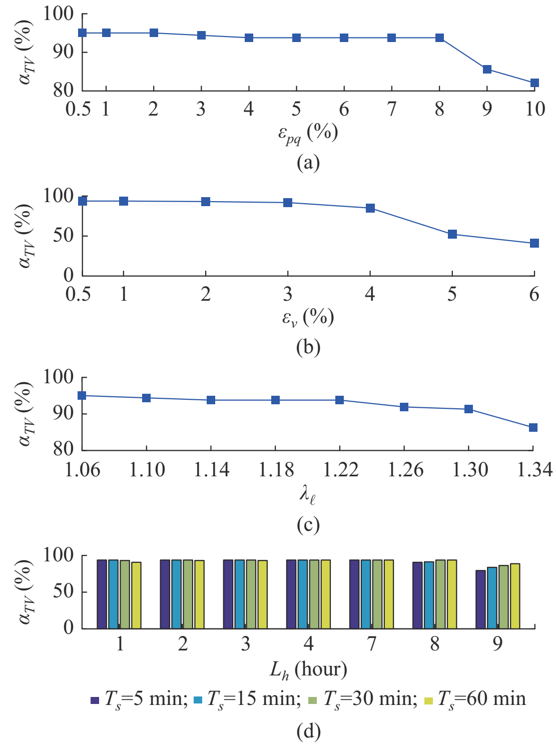

Fig. 12. Result of sensitivity analysis with varying settings in modified IEEE 123-bus system. (a) ε_{pq}. (b) ε_v. (c) λ_ℓ. (d) L_h.

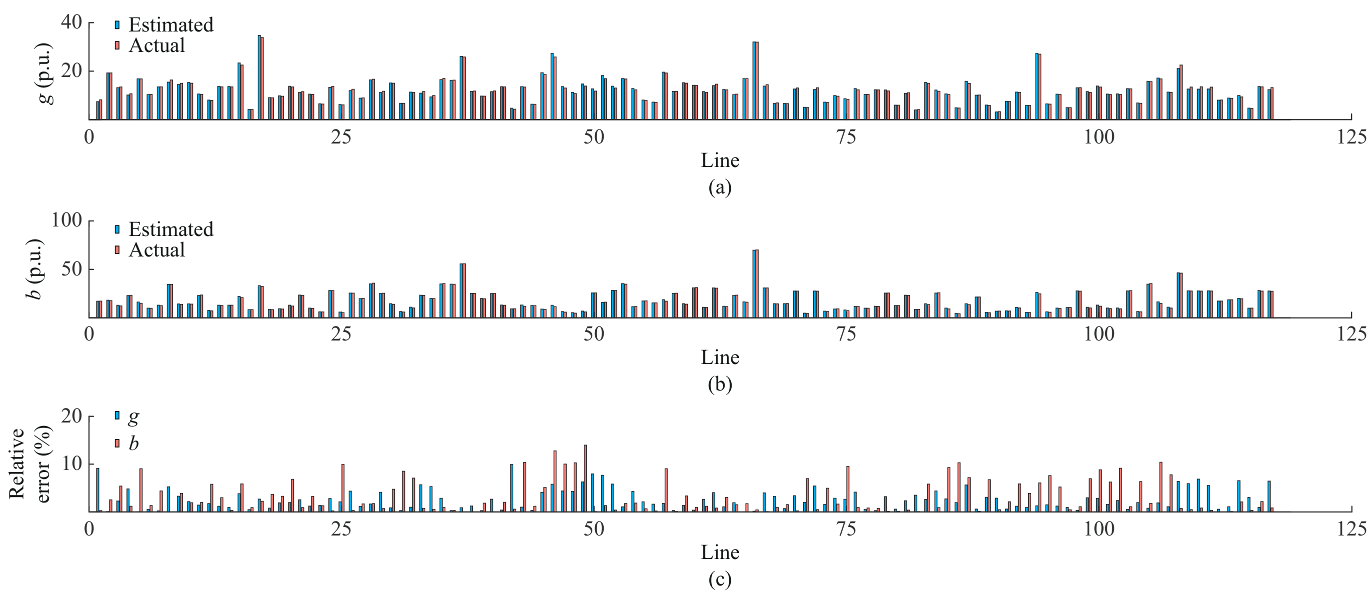

Fig. 13. Best estimates and relative error between renewed and actual values of line parameters of each line in modified IEEE 123-bus system. (a) Conductance. (b) Susceptance. (c) Relative error.

In order to further verify the validity of the proposed algorithm in large-scale distribution network, the comparison experiment is conducted with varying values of ε_{pq}, which are set to be 0.5%, 1.0%, 3.0%, 5.0%, and 10%, respectively. The result is presented in Table II. In Table II, it is clear that the FSAP-SNR achieves better estimation results than FSAP. It implies that the result of FSAP with fixed iteration step is not enough for the complex distribution network. All line parameters must be fine-tuned in combination with SNR to make the results more accurate. Thus, FSAP-SNR is preferred for large-scale distribution network.

TABLE II
RESULT OF COMPARISON EXPERIMENTS IN MODIFIED IEEE 123-BUS SYSTEM

ε_{pq} (%)	FSAP		FSAP-SNR	
	MAPE(*g*)	*MAPE*(*b*)	*MAPE*(*g*)	*MAPE*(*b*)
0.5	3.085	3.670	2.577	3.199
1.0	3.099	3.685	2.625	3.358
3.0	3.101	3.725	2.685	3.485
5.0	3.104	3.797	2.742	3.632
10.0	3.106	3.810	2.787	3.650

3) Line Aging Assessment

The risk assessment is employed to assess the aging severity of each line in the modified topology in Fig. 4. The result is shown in Fig. 14. V_{aw} is set to be 0.12, and there are 5 lines exceeding V_{aw}, which needs to be alerted.

D. Discussion

Combining the results of the modified IEEE 33-bus and 123-bus systems, the FSAP displays its outstanding and robust performance in fast parameter estimation. In small distribution network, the accuracy of FASP is acceptable in line parameter estimation. In the large-scale distribution network, the FSAP is combined with SNR to further guarantee the accuracy of parameter estimation.

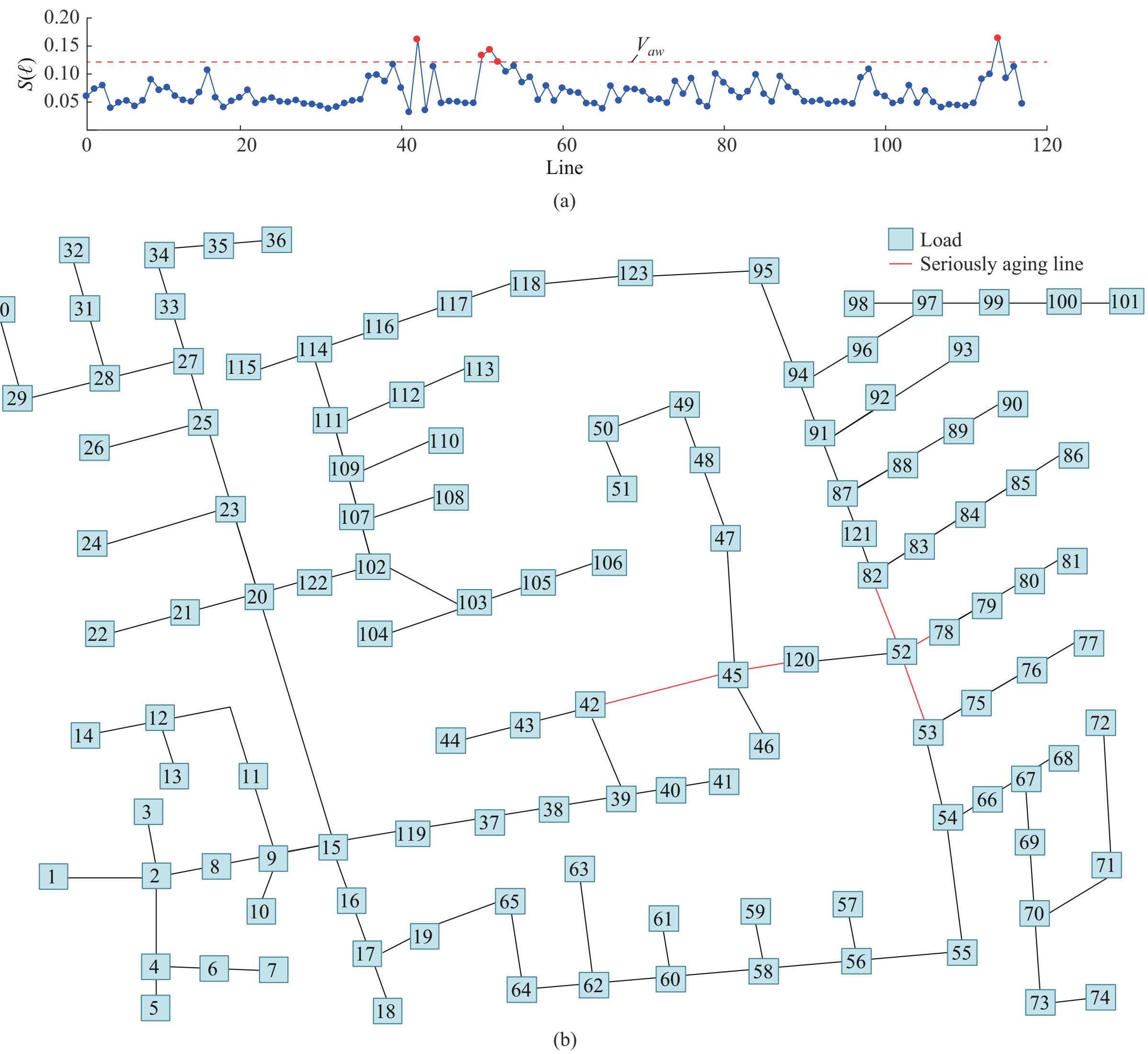

Fig. 14. Result of line aging assessment of modified IEEE 123-bus system. (a) $S(\ell)$. (b) Topology structure.

Especially, when the voltage measurement error is high, simply employing the SNR algorithm alone may lead to non-convergence. To solve this problem, the estimated results of FSAP provide a good initial solution for SNR to benefit its convergence.

IV. CONCLUSION AND FUTURE WORK

In this paper, a novel approach is proposed for line aging assessment in the distribution network comprised of three stages: topology verification, parameter estimation, and line aging assessment.

In topology detection, the best-matched topology is determined based on the voltage magnitude and power injection data. In parameter estimation, the theoretical line parameters of the best-matched topology are renewed to best fit the actual measurement data based on the proposed FSAP-SNR approach. In line aging assessment, the risk assessment technology is utilized to quantify the aging severity risk level of each line in the distribution network. Experiments are conducted using the dataset from the Tianjin Electric Power Company in China on the modified IEEE 33-bus and 123-bus systems. The experiment results suggest that the proposed approach could effectively conduct line aging assessment in the distribution network. Besides, case studies of parameter estimation show that FSAP is suitable for the simple distribution network. In the large-scale distribution network, FSAP-SNR is preferred.

REFERENCES

[1] Y. Wang, C. Peng, R. Liao *et al.*, "Aging risk assessment based on fuzzy logic for overhead transmission line," in *Proceedings of 46th Annual Conference of the IEEE Industrial Electronics Society*, Singapore, Oct. 2020, pp. 2606-2611.

[2] P. Musilek, J. Heckenbergerova, and M. M. I. Bhuiyan, "Spatial analysis of thermal aging of overhead transmission conductors," *IEEE Transactions on Power Delivery*, vol. 27, no. 3, pp. 1196-1204, Jul. 2012.

[3] A. Bosisio, A. Berizzi, E. Amaldi *et al.*, "Optimal feeder routing in urban distribution networks planning with layout constraints and losses," *Journal of Modern Power Systems and Clean Energy*, vol. 8, no. 5, pp. 1005-1014, Sept. 2020.

[4] H. Long, C. Chen, W. Gu *et al.*, "A data-driven combined algorithm for abnormal power loss detection in the distribution network," *IEEE Access*, vol. 8, pp. 24675-24686, Jan. 2020.

[5] G. Montanari, D. Fabiani, and F. Ciani, "Partial discharge and aging of AC cable systems under repetitive voltage transient supply," in *Proceedings of 2016 IEEE Electrical Insulation Conference (EIC)*, Montreal, Canada, Aug. 2016, pp. 379-382.

[6] L. Förstel and L. L. Lampe, "Grid diagnostics: monitoring cable aging using power line transmission," in *Proceedings of 2017 IEEE International Symposium on Power Line Communications and Its Applications (ISPLC)*, Madrid, Spain, Apr. 2017, pp. 1-6.

[7] L. Ding, "Research on the influence of aging and high resistance grounding fault on 10 kV line," *Jiangxi Electric Power*, vol. 44, no. 8, pp. 35-38, Aug. 2020.

[8] L. Chen, X. Bian, S. Wan *et al.*, "Influence of temperature character of AC aged conductor on current carrying capacity," *High Voltage Engineering*, vol. 40, no. 5, pp. 1499-1506, May 2014.

[9] M. Buhari, V. Levi, and S. K. Awadallah, "Modelling of ageing distribution cable for replacement planning," *IEEE Transactions on Power Systems*, vol. 31, no. 5, pp. 3996-4004, Nov. 2015.

[10] P. Musilek, J. Heckenbergerova, and M. M. I. Bhuiyan, "Spatial analysis of thermal aging of overhead transmission conductors," *IEEE Transactions on Power Delivery*, vol. 27, no. 3, pp. 1196-1204, Jul. 2012.

[11] Y. Guo, R. Chen, J. Shi *et al.*, "Determination of the power transmission line ageing failure probability due to the impact of forest fire," *IET Generation, Transmission & Distribution*, vol. 12, pp. 3812-3819, Sept. 2018.

[12] D. Pál, Ľ. Beňa, J. Urbanský *et al.*, "The impact of reconfiguration on power losses in smart networks," in *Proceedings of 2020 21st International Scientific Conference on Electric Power Engineering (EPE)*, Prague, Czech, Oct. 2020, p. 9269189.

[13] G. Cavraro, A. Bernstein, V. Kekatos *et al.*, "Real-time identifiability of power distribution network topologies with limited monitoring," *IEEE Control Systems Letters*, vol. 4, no. 2, pp. 325-330, Apr. 2020.

[14] R. Arghandeh, M. Gahr, A. von Meier *et al.*, "Topology detection in microgrids with micro-synchrophasors," in *Proceedings of 2015 IEEE PES General Meeting*, Denver, USA, Sept. 2015, p. 7286053.

[15] G. Cavraro, V. Kekatos, and S. Veeramachaneni, "Voltage analytics for power distribution network topology verification," *IEEE Transactions on Smart Grid*, vol. 10, no. 1, pp. 1058-1067, Jan. 2019.

[16] R. A. Sevlian, Y. Zhao, R. Rajagopal *et al.*, "Outage detection using load and line flow measurements in power distribution systems," *IEEE Transactions on Power Systems*, vol. 33, no. 2, pp. 2053-2069, Mar. 2018.

[17] J. Yu, Y. Weng, and R. Rajagopal, "PaToPa: a data-driven parameter and topology joint estimation framework in distribution grids," *IEEE Transactions on Power Systems*, vol. 33, no. 4, pp. 4335-4347, Jul. 2018.

[18] J. Zhang, Y. Wang, Y. Weng *et al.*, "Topology identification and line parameter estimation for non-PMU distribution network: a numerical method," *IEEE Transactions on Smart Grid*, vol. 11, no. 5, pp. 4440-4453, Sept. 2020.

[19] G. Cavraro and V. Kekatos, "Inverter probing for power distribution network topology processing," *IEEE Transactions on Control of Network Systems*, vol. 6, no. 3, pp. 980-992, Sept. 2019.

[20] S. Taheri, V. Kekatos, and G. Cavraro, "An MILP approach for distribution grid topology identification using inverter probing," in *Proceedings of IEEE PowerTech*, Milan, Italy, Jun. 2019, p. 8810900.

[21] M. Z. A. Bhuiyan, G. J. Anders, J. Philhower *et al.*, "Review of static risk-based security assessment in power system," *IET Cyber-Physical Systems: Theory & Applications*, vol. 4, no. 3, pp. 233-239, Sept. 2019.

[22] L. Li, L. Liu, H. Wu *et al.*, "Identification of critical hidden failure line based on state-failure-network," *Journal of Modern Power Systems and Clean Energy*, vol. 10, no. 1, pp. 40-49, Jan. 2022.

[23] H. Jia, W. Qi, Z. Liu *et al.*, "Hierarchical risk assessment of transmission system considering the influence of active distribution network," *IEEE Transactions on Power Systems*, vol. 30, no. 2, pp. 1084-1093, Mar. 2015.

[24] C. Wang, C. Yan, G. Li *et al.*, "Risk assessment of integrated electricity and heat system with independent energy operators based on Stackelberg game," *Energy*, vol. 198, p. 117349, May 2020.

Zhi Wu received the B.Eng. degree in mathematics from Southeast University, Nanjing, China, in 2009, the M. Sc. degree in electrical engineering from the School of Electrical Engineering, Southeast University, in 2012, and the Ph.D. degree from the University of Birmingham, Birmingham, UK, in 2016. He is currently an Associate Professor with Southeast University. His research interests include renewable energy, and planning and optimization techniques.

Huan Long received the B. Eng. degree from Huazhong University of Science and Technology, Wuhan, China, in 2013, and the Ph. D. degree from the City University of Hong Kong, Hong Kong, China, in 2017. She is currently an Associate Professor with the School of Electrical Engineering, Southeast University, Nanjing, China. Her research interests include artificial intelligence applied in modeling, optimizing, monitoring renewable energy system and power system.

Chang Chen received the B.S. degree in Department of Automation from Nanjing University of Aeronautics and Astronautics, Nanjing, China, in 2018, and the M.S. degree in electrical engineering from Southeast University, Nanjing, China, in 2021. She is currently with State Grid Jiangsu Electric Power Company Ltd., Maintenance Branch Company, Nanjing, China. Her research interest includes power system analysis.